

# A Fast Post-Training Pruning Framework for Transformers

Woosuk Kwon<sup>1,\*</sup>, Sehoon Kim<sup>1,\*</sup>, Michael W. Mahoney<sup>1</sup>

Joseph Hassoun<sup>2</sup>, Kurt Keutzer<sup>1</sup>, Amir Gholami<sup>1</sup>

<sup>1</sup>University of California, Berkeley <sup>2</sup>Samsung Semiconductor, Inc.

{woosuk.kwon, sehoonkim, mahoneymw, keutzer, amirgh}@berkeley.edu  
j.hassoun@samsung.com

**Abstract**—Pruning is an effective way to reduce the huge inference cost of large Transformer models. However, prior work on model pruning requires retraining the model. This can add high cost and complexity to model deployment, making it difficult to use in many practical situations. To address this, we propose a fast post-training pruning framework for Transformers that does not require any retraining. Given a resource constraint and a sample dataset, our framework automatically prunes the Transformer model using structured sparsity methods. To retain high accuracy without retraining, we introduce three novel techniques: (i) a lightweight mask search algorithm that finds which heads and filters to prune based on the Fisher information; (ii) mask rearrangement that complements the search algorithm; and (iii) mask tuning that reconstructs the output activations for each layer. We apply our method to BERT<sub>BASE</sub> and DistilBERT, and we evaluate its effectiveness on GLUE and SQuAD benchmarks. Our framework achieves up to 2.0 $\times$  reduction in FLOPs and 1.56 $\times$  speedup in inference latency, while maintaining < 1% loss in accuracy. Importantly, our framework prunes Transformers in less than 3 minutes on a single GPU, which is over two orders of magnitude faster than existing pruning approaches that retrain. Our code is publicly available.

## I. INTRODUCTION

In recent years, the Transformer [74] has become a *de facto* standard model architecture in Natural Language Processing [4, 11, 43], and it is becoming common in Computer Vision [13, 45, 73] and Speech Recognition [2, 7, 24] as well. However, efficient deployment of Transformer architectures has been challenging due to their large model size and high latency. To address this, structured pruning has become a promising technique for efficient Transformer deployment.

While prior work on pruning Transformers substantially reduces inference time, it is often difficult to use in

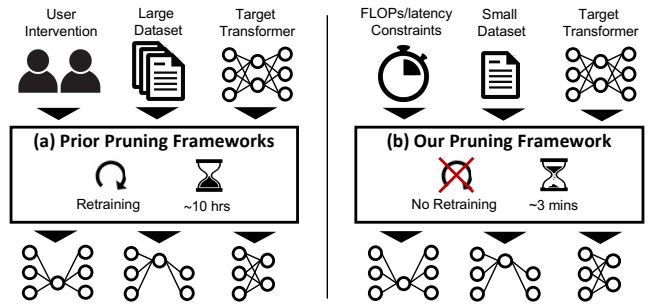


**Fig. 1:** (a) Prior pruning frameworks require additional training on the entire training set and involve user intervention for hyperparameter tuning. This complicates the pruning process and requires a large amount of time (e.g., ~10 hours). (b) Our pruning framework does not require retraining. It outputs pruned Transformer models satisfying the FLOPs/latency constraints within much less time (e.g., ~3 minutes), without user intervention.

practice for several reasons. First, previous approaches require retraining the pruned model and/or jointly learning the pruning configurations during training. For instance, Block Movement Pruning [36] increases the training time by 10 $\times$  for pruning. Such additional training adds significant computational overhead, given the large training cost of Transformers. Second, previous methods add many moving parts to the model deployment process. Pruning pipelines are often complex and involve additional hyperparameter tuning. For instance, ROSITA [44] uses a three-stage knowledge distillation [22] with sophisticated pruning schedules. Such techniques demand significant engineering efforts for reproducing and debugging, which impedes their adoption in production pipelines. Third, these previous methods do not directly adapt to the users' FLOPs/latency constraints. They either rely on vague regularization hyperparameters or fixed architectures selected independently of the user settings. This can

\*Equal contribution.

result in sub-optimal models not tailored for the given constraint and target hardware.

To address these limitations, we propose a fast *post-training pruning* framework for Transformers that does not require any retraining of the models. As illustrated in Figure 1, our framework takes as input a Transformer model, a sample dataset, and a FLOPs/latency constraint. It then outputs a pruned Transformer model that can be deployed immediately. By avoiding expensive retraining, the end-to-end compression pipeline can be extremely fast and simplified, typically in a few minutes, without any user interventions that complicate the whole process.

Indeed, post-training compression has been widely studied for quantization, and it gained considerable attention in both academia and industry [3, 26, 91]. Although quantization-aware training methods achieve higher compression rates in general, post-training quantization (PTQ) has often been more preferred in practice due to its retraining-free advantage. PTQ allows quantization to happen seamlessly when deploying models through the various frameworks such as TensorRT [53], TFLite [17], and OpenVINO [28]. Similar to these PTQ frameworks, our framework provides an out-of-the-box tool that enables pruning of Transformers without engineering efforts.

Our contributions can be summarized as follows:

- We propose a novel post-training pruning framework for Transformers that does not require model retraining. To retain accuracy without retraining, our framework consists of three stages of: (i) the *mask search* process guided by the Fisher information matrix to find which heads/filters to prune (Section IV-A); (ii) the *mask rearrangement* process that rearranges the pruned heads/filters by capturing intra-layer interactions (Section IV-B); and (iii) the *mask tuning* process that adjusts the mask variables to ensure that the output signal is recovered for each layer (Section IV-C).
- We extensively test our framework by applying it to BERT<sub>BASE</sub> and DistilBERT on GLUE and SQuAD tasks (Section V-B). With 1% of accuracy drop, our framework reduces 30–50% of the original FLOPs (Figure 4), resulting in up to 1.56× speedup on an NVIDIA V100 GPU (Table I).
- We show that our method achieves comparable or even better FLOPs-accuracy trade-off than prior structured pruning methods *without* retraining (Section V-C, Figure 5). Our end-to-end pruning finishes in only 39 and 135 seconds on average for GLUE and SQuAD (Section V-D, Table IV), which is over 100× faster than the retraining methods.

- We open-source our framework at GitHub<sup>1</sup>, along with the model checkpoints used in our experiments.

## II. RELATED WORKS

**Efficient Transformers.** In order to improve inference speed and reduce memory footprint of Transformers, multiple different approaches have been proposed. These can be broadly categorized as follows: (i) efficient architecture design [27, 34, 37, 69, 79, 85]; (ii) hardware-software co-design [18, 19, 70, 78]; (iii) knowledge distillation [30, 60, 68, 80]; (iv) quantization [32, 63, 89, 90]; (v) neural architecture search [6, 64, 65, 77, 86, 88]; and (vi) pruning. Here, we focus only on pruning and briefly discuss the related works.

**Transformers Pruning.** Pruning has been a popular choice for reducing unimportant weights and redundant parts in Transformers. Pruning can be broadly categorized into unstructured and structured pruning. For unstructured pruning, magnitude-based pruning [16], the lottery-ticket hypothesis [8, 9, 15, 55], movement pruning [61] have been explored for Transformers. While these methods compress the model size, commodity hardware cannot take advantage of the unstructured sparsity for speedup.

For this reason, a number of structured pruning methods have been introduced to remove structured sets of parameters. For example, [48, 75] drop attention heads in multi-head attention layers. Another thread of work prunes entire Transformer blocks based on a simple heuristic [59] or an adaptive training using a layer-wise dropout method [14]. Relatedly, [81] structurally prunes weight matrices via low-rank factorization and  $l_0$  regularization; [31, 41] attempt to jointly prune attention heads and filters of weight matrices; and [23, 46] take a step further by dynamically determining the pruning configurations at run time. Recent block pruning schemes chunk weight matrices into blocks and prune them based on group Lasso optimization [40], adaptive regularization [87], and movement pruning [36].

While the structured pruning techniques have achieved high compression rates and speedups, the improvement largely attributes to retraining of the models during or after pruning, often combined with knowledge distillation. However, model retraining introduces several practical problems. Most notably, retraining in general increases training time significantly. For instance, Block Movement Pruning [36], a state-of-the-art structured Transformer pruning method, requires 10× longer training time than normal fine-tuning. In addition, the extra hyperparameters

<sup>1</sup><https://github.com/WoosukKwon/retraining-free-pruning>

introduced by the pruning methods add additional moving parts and lead to increased training cost.

**Post-training Model Compression.** Post-training compression methods have been widely studied in quantization. These methods, categorized as post-training quantization (PTQ), perform quantization without any retraining, thereby minimizing the training cost and user intervention. Multiple approaches have been proposed for PTQ in order to mitigate the accuracy degradation without retraining, including analytic computation of optimal clipping ranges [3], outlier channel splitting [91], and adaptive rounding methods [26, 51].

Although not as much as for quantization, post-training schemes have also been explored for unstructured [25, 71] and structured pruning. For structured pruning, [67] proposes to detect and merge similar convolution filters iteratively, and [33] compensates for the information loss due to pruning by merging similar neurons based on cosine distance. While these methods are effective for CNNs, their applicability is limited to models with simple architectures, and they rely on the characteristics of ReLU nonlinearity [25, 33]. Hence, the prior methods cannot be extended to the general Transformer architectures.

### III. OVERVIEW

#### A. Background

**Transformer Architecture.** In this paper, we focus on the pruning of encoder-based Transformer [74] models, especially the BERT [11] architecture family. BERT is a stack of homogeneous Transformer encoder blocks, each of which consists of a multi-head attention (MHA) layer followed by a point-wise Feed-Forward Network (FFN) layer. Specifically, an MHA layer consists of  $H$  independently parameterized attention heads:

$$\text{MHA}(\mathbf{x}) = \sum_{i=1}^H \text{Att}_i(\mathbf{x}), \quad \mathbf{x}_{\text{MHA}} = \text{LN}(\mathbf{x} + \text{MHA}(\mathbf{x})),$$

where  $\text{Att}$  is a dot product attention head,  $\text{LN}$  is layer normalization, and  $\mathbf{x}$  is the input sequence. The output of the MHA layer is then fed into the FFN layer, which consists of  $N$  filters:

$$\begin{aligned} \text{FFN}(\mathbf{x}) &= \left( \sum_{i=1}^N \mathbf{W}_{:,i}^{(2)} \sigma(\mathbf{W}_{i,:}^{(1)} \mathbf{x} + \mathbf{b}_i^{(1)}) \right) + \mathbf{b}^{(2)}, \\ \mathbf{x}_{\text{out}} &= \text{LN}(\mathbf{x}_{\text{MHA}} + \text{FFN}(\mathbf{x}_{\text{MHA}})), \end{aligned}$$

where  $\mathbf{W}^{(1)}, \mathbf{W}^{(2)}, \mathbf{b}^{(1)}$  and  $\mathbf{b}^{(2)}$  are the FFN parameters, and  $\sigma$  is the activation function, typically GELU [21]. Note that  $(H, N)$  is  $(12, 3072)$  for BERT<sub>BASE</sub>, and  $(16,$

4096) for BERT<sub>LARGE</sub>. We also denote  $L$  as the number of Transformers layers.

**Granularity of Pruning and Notations.** Our framework considers the structured pruning of both heads in MHA and filters in FFN layers. We do not prune the embedding and the final classifier, as computation of those layers takes a negligible portion of the total inference latency. Since our pruning framework always produces a smaller dense architecture, the model can be readily accelerated without the need for specific hardware logic, which is often required to gain latency speedup for unstructured sparsity.

For mathematical simplicity, we introduce mask variables associated with the outputs of heads and filters:

$$\begin{aligned} \text{MHA}(\mathbf{x}; \mathbf{m}_l^{\text{MHA}}) &= \sum_{i=1}^H m_{l,i}^{\text{MHA}} \circ \text{Att}_i(\mathbf{x}), \\ \text{FFN}(\mathbf{x}; \mathbf{m}_l^{\text{FFN}}) &= \left( \sum_{i=1}^N m_{l,i}^{\text{FFN}} \circ \mathbf{W}_{:,i}^{(2)} \sigma(\mathbf{W}_{i,:}^{(1)} \mathbf{x} + \mathbf{b}_i^{(1)}) \right) + \mathbf{b}^{(2)}, \end{aligned}$$

where  $\mathbf{m}_l^{\text{MHA}} \in \mathbb{R}^H$  and  $\mathbf{m}_l^{\text{FFN}} \in \mathbb{R}^N$  are the mask variables for MHA and FFN in the  $l$ -th layer, respectively, and  $m_{l,i}^{\text{MHA}}$  and  $m_{l,i}^{\text{FFN}}$  are their  $i$ -th elements. Furthermore,  $\circ$  denotes Hadamard product. Originally, the mask variables are initialized to 1. Zeroing out a mask variable is equivalent to pruning a head/filter associated with it. That is, setting  $m_{l,i}^{\text{MHA}}$  and  $m_{l,i}^{\text{FFN}}$  as zero is equivalent to pruning the  $i$ -th head and filter, respectively. This process is illustrated in Figure 2 (Top).

Overall, there are  $HL$  head mask variables and  $NL$  filter mask variables, summing up to  $(H+N)L$  number of total mask variables in a Transformer model. To simplify notations, we additionally define  $\mathbf{m}^{\text{MHA}} \in \mathbb{R}^{HL}$ ,  $\mathbf{m}^{\text{FFN}} \in \mathbb{R}^{NL}$ , and  $\mathbf{m} \in \mathbb{R}^{(H+N)L}$  as the flattened vectors of the head, filter, and total mask variables, respectively, across all layers. In what follows, we discuss how to find the optimal sparse masks under a given cost constraint and how to adjust their values to recover accuracy.

#### B. Framework Overview

Figure 1(b) and Figure 2 (Bottom) illustrate the overview of our framework.

**Inputs.** Our framework has 3 inputs: a Transformer model; a sample dataset; and a resource constraint. The input Transformer model should be fine-tuned for a downstream task. The sample dataset is a small partition of the training dataset (typically 1–2K examples) of the downstream task. The resource constraint can be given either as the number of floating point operations (FLOPs)

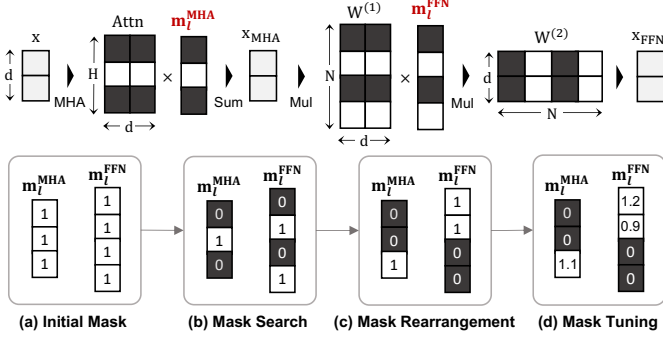


**Fig. 2:** (Top row) An overview of a pruned Transformer layer (residual connections and LayerNorms are omitted for simplicity) where the number of heads ( $H$ ) and filters ( $N$ ) are 3 and 4, respectively. The black entries indicate pruned heads and filters by zeroing out the associated mask variables. (Bottom row) Overview of our framework. (a) The mask variables are initialized as 1. Then they undergo the 3-stage pipeline of (b) mask search (Section IV-A), (c) rearrangement (Section IV-B), and (d) tuning (Section IV-C).

or as an actual latency on target hardware. In the later case, we further assume that a latency lookup table for the target hardware is provided.

**Compression Pipeline.** As illustrated in Figure 2, our framework consists of 3 stages: Fisher-based mask search; Fisher-based mask rearrangement; and mask tuning. During the *Fisher-based mask search* stage (Section IV-A), we search for a binary mask applied to the heads and filters by incorporating the Fisher information of the mask variables. Intuitively, the mask variables with relatively higher Fisher information are considered more important, and they should be less likely to be pruned [38, 42, 50]. As finding the optimal mask that minimizes the Fisher information loss is intractable using the full Fisher matrix, we propose a lightweight search algorithm that finds the optimal mask under reasonable approximations. Second, in the *Fisher-based mask rearrangement* stage (Section IV-B), the framework modifies the searched mask patterns in a layer-wise manner to better take into account the intra-layer interactions of the mask variables. Lastly, in the *mask tuning* stage (Section IV-C), the framework tunes the nonzero mask variables to recover the accuracy drop by reconstructing the layer-wise output signal.

#### IV. METHODOLOGY

We pose the pruning problem as finding a binary mask to zero out a particular head or filter. After

finding the initial set of mask variables, we then allow adaptation/tuning of the remaining masks variables to avoid changes in the output norm of a layer. This process is done without any retraining of the model.

Note that the number of the mask variables is much less than the number of parameters in a Transformer (e.g., 37K vs. 110M in case of BERT<sub>BASE</sub>). This allows the framework to use only a small number of examples without overfitting to a sample dataset, and thus to be extremely fast compared to the retraining-based pruning methods which typically uses the entire training dataset. As the framework keeps the model “as is” and only decides the mask variables, we henceforth regard the model parameters as constants and consider the mask variables as the only parameters for our pruning problem.

**Problem Formulation.** We formulate Transformer pruning as a constrained optimization problem on the mask  $m$ :

$$\arg \min_m \mathcal{L}(m) \quad \text{s.t.} \quad \text{Cost}(m) \leq C \quad (1)$$

where  $\mathcal{L}$  denotes the loss function, Cost is the FLOPs/latency of the architecture pruned by the mask, and  $C$  is the given FLOPs/latency constraint. Unfortunately, such a problem is generally intractable as Cost is usually a function of  $l_0$ -norm of the mask  $m$ , which is non-differentiable. Thus, in what follows, we introduce several assumptions and approximations to simplify the problem.

We start by approximating the loss function using the second-order Taylor expansion around the initial mask  $\mathbb{1}$ :

$$\mathcal{L}(m) = \mathcal{L}(\mathbb{1} - (\mathbb{1} - m)) \quad (2)$$

$$\approx \mathcal{L}(\mathbb{1}) - \mathbf{g}^\top(\mathbb{1} - m) + \frac{1}{2}(\mathbb{1} - m)^\top \mathbf{H}(\mathbb{1} - m) \quad (3)$$

$$\approx \mathcal{L}(\mathbb{1}) + \frac{1}{2}(\mathbb{1} - m)^\top \mathbf{H}(\mathbb{1} - m), \quad (4)$$

where  $\mathbf{g} = \mathbb{E}[\frac{\partial}{\partial m} \mathcal{L}(\mathbb{1})]$  and  $\mathbf{H} = \mathbb{E}[\frac{\partial^2}{\partial m^2} \mathcal{L}(\mathbb{1})]$ . Eq. 4 is deduced from an assumption that the model has converged to a local minima, where the gradient term is close to 0 [38]. As  $\mathcal{L}(\mathbb{1})$  is a constant, we can rewrite the optimization objective as follows:

$$\arg \min_m \mathcal{L}(m) \approx \arg \min_m (\mathbb{1} - m)^\top \mathbf{H}(\mathbb{1} - m). \quad (5)$$

Eq. 5 shows that the optimal mask is determined by the Hessian of the loss with respect to the mask variables. Since forming the exact Hessian matrix explicitly is infeasible, we approximate the Hessian  $\mathbf{H}$  with the empirical Fisher information matrix  $\mathcal{I}$  of the mask variables:

$$\mathcal{I} := \frac{1}{|\mathcal{D}|} \sum_{(x,y) \in \mathcal{D}} \left( \frac{\partial}{\partial m} \mathcal{L}(x, y; \mathbb{1}) \right) \left( \frac{\partial}{\partial m} \mathcal{L}(x, y; \mathbb{1}) \right)^\top, \quad (6)$$

**Algorithm 1** Mask Search with a FLOPs Constraint

**Input:** FLOPs constraint  $C$ , diagonal Fisher information matrix  $\mathcal{I}$

---

```

1: for  $n = 0$  to  $HL$  do                                 $\triangleright$  # remaining heads
2:    $k_1 = HL - n$                                  $\triangleright$  # heads to prune
3:    $HI =$  indices of  $k_1$  least important heads
4:    $f = \lfloor (C - nF_{\text{head}})/F_{\text{filter}} \rfloor$      $\triangleright$  # remaining filters
5:    $k_2 = NL - f$                                  $\triangleright$  # filters to prune
6:    $FI =$  indices of  $k_2$  least important filters
7:    $S[n] = \sum_{i \in HI \cup FI} \mathcal{I}_{ii}$ 
8:    $R[n] = (HI, FI)$ 
9: end for
10:   $n^* = \arg \min_n S[n]$                        $\triangleright$  optimal # remaining heads
11:   $HI^*, FI^* = R[n^*]$                           $\triangleright$  indices of heads/filters to prune
12:  Initialize  $m^{\text{MHA}}$  and  $m^{\text{FFN}}$  as 1
13:   $m^{\text{MHA}}[HI^*] = 0$                           $\triangleright$  prune the selected heads
14:   $m^{\text{FFN}}[FI^*] = 0$                           $\triangleright$  prune the selected filters

```

---

**Output:**  $m^* = (m^{\text{MHA}}, m^{\text{FFN}})$

where  $\mathcal{D}$  is the sample dataset and  $(x, y)$  is a tuple of an input example and its label.

### A. Fisher-Based Mask Search

**Diagonal Approximation of Fisher Information Matrix.** It is not straightforward to solve the optimization objective in Eq. 5 using the full empirical Fisher information matrix  $\mathcal{I}$ . Thus, we first make a simple assumption that  $\mathcal{I}$  is *diagonal*. This further simplifies Eq. 5 as follows:

$$\arg \min_m \mathcal{L}(m) \approx \arg \min_m \sum_i (1 - m_i)^2 \mathcal{I}_{ii}, \quad (7)$$

Since we restrict the possible mask values to either 0 or 1, the following can be derived from Eq. 7:

$$\arg \min_m \mathcal{L}(m) \approx \arg \min_m \sum_{i \in Z(m)} \mathcal{I}_{ii}, \quad (8)$$

$$\text{where } Z(m) := \{i \mid m_i = 0\}. \quad (9)$$

We can interpret the diagonal element of  $\mathcal{I}$  as the *importance score* of the head/filter associated with each mask variable, and Eq. 8 as a process of minimizing the total importance scores of the pruned heads and filters. Such an importance score has also been introduced in [50, 72] to guide pruning.

**Solving FLOPs-constrained Problem.** We need to solve Eq. 8 given a cost constraint. For a given target FLOP cost, denoted by  $C$ , we can formulate the binary mask search problem as follows:

$$\arg \min_m \sum_{i \in Z(m)} \mathcal{I}_{ii}, \quad (10)$$

$$\text{s.t. } F_{\text{head}} \|m^{\text{MHA}}\|_0 + F_{\text{filter}} \|m^{\text{FFN}}\|_0 \leq C, \quad (11)$$

where  $F_{\text{head}} \in \mathbb{R}$  and  $F_{\text{filter}} \in \mathbb{R}$  are the FLOPs for computing a head and a filter, respectively. Note that

the number of FLOPs of a head/filter is constant across all layers. While such an optimization problem can be generally solved by a knapsack algorithm [1, 62], the following observations allow a simpler and faster solution: (1) having more heads and filters unpruned always optimizes Eq. 10 since the diagonal elements of  $\mathcal{I}$  are non-negative; and (2) if a certain number of heads needs to be pruned, they should be the ones with the lowest importance scores because each head accounts for the same amount of FLOPs. The same statement also holds for pruning filters. These lead to our mask search algorithm described in Algorithm 1.

Algorithm 1 partitions the solution space by the number of remaining heads in the pruned architecture ( $n$  in line 1). For each  $n$ , by observation (1), the number of remaining neurons should be as line 4. Then by observation (2) the heads/filters with the lowest important scores are selected to be pruned.  $S[n]$  is the evaluation of Eq. 10 with this mask. When the loop terminates, the output is the mask with the smallest  $S[n]$ . In Section A, we prove that the output mask  $m^*$  of Algorithm 1 is optimal. That is, any other mask  $m$  satisfying the given FLOPs constraint will have a higher loss:

$$\sum_{i \in Z(m^*)} \mathcal{I}_{ii} \leq \sum_{i \in Z(m)} \mathcal{I}_{ii}. \quad (12)$$

**Solving Latency-constrained Problem.** If the cost constraint is given in terms of actual latency on target hardware, we have a new cost constraint formula in the optimization target in Eq. 10:

$$\sum_{l=1}^L \text{LAT}(m_l^{\text{MHA}}) + \sum_{l=1}^L \text{LAT}(m_l^{\text{FFN}}) \leq C, \quad (13)$$

where the function  $\text{LAT}$  indicates the latency of a MHA/FFN layer after pruning. We assume that a latency lookup table on the target hardware is provided so that evaluating  $\text{LAT}$  takes very small overhead.

Unfortunately, the problem with a latency constraint is more challenging than the problem with a FLOPs constraint, and it cannot be solved by directly applying Algorithm 1. This is because  $\text{LAT}$  may *not* be linear to the number of remaining heads or filters after pruning [56], as shown in Figure 3 (Left). We can interpret this as follows: (1) with a sufficient number of heads/filters in a layer, the hardware resources such as parallel cores can be fully utilized, resulting in latency roughly proportional to the number of heads/filters; and (2) otherwise, the hardware resources are underutilized and a constant overhead dominates the latency [35, 47]. Thus, pruning

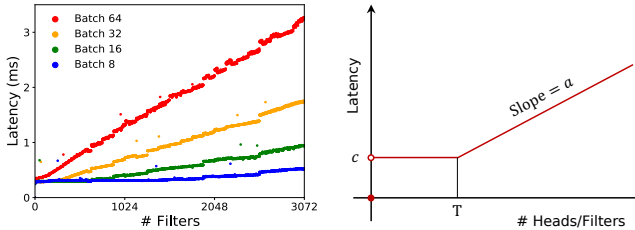


**Fig. 3:** (Left) Real latency of a single FFN layer with different numbers of remaining filters, measured on an NVIDIA V100 GPU with input sequence length 64. (Right) Schematic plot for the approximated latency as a piecewise linear function.

more heads/filters below a certain threshold does not translate into actual speedup.

Based on the above analysis, we approximate LAT as a piece-wise linear function as in Figure 3 (Right) such that  $\text{LAT}(m_l)$  is 0 if  $\|m_l\|_0 = 0$ ,  $c$  if  $0 < \|m_l\|_0 \leq T$ , and  $a(\|m_l\|_0 - T) + c$  if  $\|m_l\|_0 > T$ , where  $c \in \mathbb{R}$  is the constant overhead,  $T \in \mathbb{N}$  is the threshold number of heads/filters that the latency starts to be linear, and  $a \in \mathbb{R}$  is the slope of the linear part. This can be easily obtained by fitting the actual latency in the lookup table with the minimum mean squared error.

This LAT approximation allows us to extend Algorithm 1 to solving the problems with latency constraints. The core idea is to consider separately the constant part of LAT and the linear part of LAT; after handling the constant part, we can apply the Algorithm 1 to the linear part. This method guarantees the optimal solution for all cases only if we do not consider the case of pruning entire layers. As we observe that dropping an entire layer leads to significant accuracy drop without retraining, we believe our algorithm finds optimal solutions in most cases. The detailed modification to Algorithm 1 is described in Section B.

### B. Fisher-based Mask Rearrangement

**Block Diagonal Approximation of Fisher Information Matrix.** Although it simplifies the problem, the diagonal assumption in Section IV-A alone might not find the best solution, as it does not take into account the interactions between different mask variables. We can capture the interactions by using a block diagonal approximation to the Fisher operator. Here a block corresponds to a MHA layer or a FFN layer. However, the block diagonal approximation results in a hard-to-optimize binary mask search problem. To alleviate this problem, we use the results from the previous step to

warm start the optimization problem with the block-diagonal approximation. That is, given the mask  $m^*$  obtained in Section IV-A, we constrain  $\|m_l\|_0$  to be equal to  $\|m_l^*\|_0$  for all layers  $l$ .

Given the two assumptions, that (i) there is no interaction between the mask variables in different layers (i.e., the block diagonal approximation), and (ii) the number of pruned heads/filters are pre-determined for each layer (i.e., warm-start), Eq. 5 breaks down to a set of layer-wise optimization problems, as follows based on the derivation in Section C:

$$\hat{m}_l = \arg \min_{m_l} (\mathbb{1} - m_l)^T \mathcal{I}_l (\mathbb{1} - m_l), \quad (14)$$

where  $\mathcal{I}_l$  is the  $l$ -th diagonal block of  $\mathcal{I}$ . This can be approximately solved by greedily exploring the possible binary masks for  $m_l$  since  $\|m_l\|_0$  is fixed. In effect, this process *rearranges* the binary mask variables to find a better arrangement for pruning locations.

### C. Mask Tuning

In the previous two stages, the possible mask values are restricted to either 0 or 1 in order to simplify the search process. In this stage, we further relax this restriction. The *nonzero* variables in the mask  $\hat{m}$  from Section IV-B are tuned to any real values such that the pruned model recovers its accuracy.

**Layer-wise Reconstruction via Linear Least Squares.** We tune the mask variables toward minimizing the *layer-wise reconstruction error*, similarly to [20]. For each layer, we reconstruct the output activation of the original model with the remaining heads/filters in the pruned model. This can be formally written as follows:

$$\arg \min_{m_l} \|x + \text{layer}(x; m_l) - (x' + \text{layer}(x'; \mathbb{1}))\|_2^2, \quad (15)$$

where  $\text{layer}$  is the either MHA or FFN, and  $x$  and  $x'$  are the inputs to the layer of the pruned model and the original model, respectively. Note that this stage does not incur any change in model FLOPs/latency, as we only tune the non-zero valued mask variables. We show in Section D that Eq. 15 is reduced to a linear least squares problem of  $\arg \min_{m_l} \|Am_l - b\|_2^2$ , where the matrix  $A$  denotes a collection of the output activations of the model pruned by the binary mask and the vector  $b$  is the output activation of the original model.

Because the size of the matrix  $A$  can be large, our framework uses the LSMR solver in CuPy [52] to solve the linear least squares problem. For the regularization hyperparameter (i.e., `damp`) of LSMR, we fix its value to 1. Then, to increase stability, we restrict the acceptable

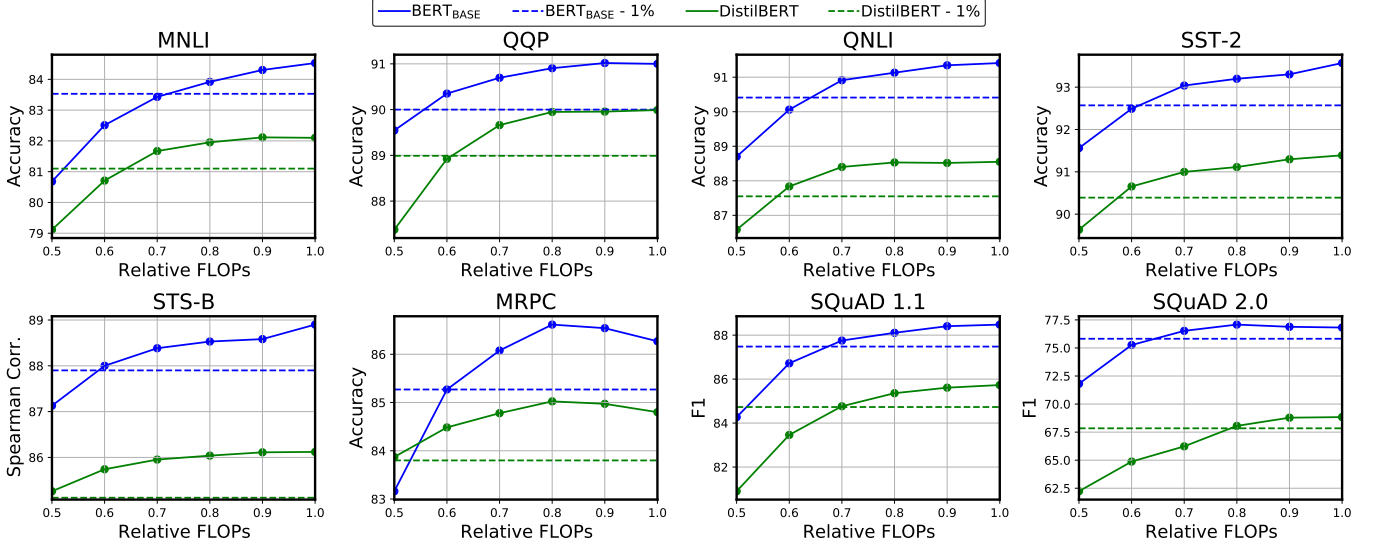


**Fig. 4:** Accuracy of our pruning method applied to  $BERT_{BASE}$  and  $DistilBERT$  with different  $FLOPs$  constraints. The dashed horizontal lines indicate 1% accuracy drop from the baseline models. Note that these results can be achieved in only 39 and 135 seconds for *GLUE* and *SQuAD* benchmarks, respectively, on a single GPU system, as described in Table IV.

range of the tuned mask variables to  $[-10, 10]$ . When the solver finds a layer mask that exceeds this range, we simply discard the mask for that layer and stop mask tuning. While the use of LSMR solver involves only two hyperparameters (i.e., *damp* and the acceptable mask range), we empirically find that these hyperparameters need not be tuned for different tasks and models. Consequently, our framework requires no user intervention in the pruning pipeline. In all of our experiments, we used the fixed hyperparameter values.

**Teacher Assistant as Reconstruction Target.** Mask tuning is analogous to knowledge distillation (KD) [22] in that a small model is optimized to mimic the behavior of a larger model. In the literature of KD, a well-known technique to bridge the gap between the student and the teacher is to introduce a *teacher assistant* (TA) [49], an intermediate-sized model that has comparable representation power to the teacher. Inspired by this, we find it effective to tune the mask variables by minimizing the reconstruction error against the intermediate representations of a TA, instead of those of the original model. In our framework, the TA is a moderately pruned model that is produced by the same search procedure in Section IV-A and Section IV-B. Specifically, when the target  $FLOPs$ /latency is  $r$  (e.g., 0.64) times that of the original model, the framework searches for a TA

model with  $\sqrt{r}$  (i.e., 0.8)  $FLOPs$ /latency, and then uses it to tune the mask of the student. As the mask search and rearrangement stages can be processed in a few seconds once the mask gradients are computed, generating a TA from the original model takes negligible time (see Table IV).

## V. EVALUATION

### A. Experimental Setup

Our framework is implemented on top of PyTorch [54] and HuggingFace Transformers [84] library. We evaluate the effectiveness of our approach using  $BERT_{BASE}$  [11] and  $DistilBERT$  [60] on *GLUE* [76] and *SQuAD* [57, 58] benchmarks. We use 2K examples from the training sets for pruning, and we evaluate the resulting models on the development sets. All of the results are averaged over the runs with 10 different seeds. More details on the experimental setup can be found in Section E.

### B. Performance Evaluation

**FLOPs.** Figure 4 shows the accuracy of  $BERT_{BASE}$  and  $DistilBERT$  with different  $FLOPs$  constraints on *GLUE* and *SQuAD* datasets. As can be seen in the plots, with only 1% of accuracy drop,  $BERT_{BASE}$  achieves 60–70% of the original  $FLOPs$  for all tasks.  $DistilBERT$  also shows a similar pattern and shows 50%  $FLOPs$

**Table I:** Latency speedup of  $BERT_{\text{BASE}}$  on an NVIDIA V100 GPU with different batch sizes. We constrain the accuracy degradation to be at most 1% from the baseline accuracy, and we report the largest speedup among those that satisfy the constraint.

Batch size	MNLI	QQP	QNLI	SST-2	STS-B	MRPC	SQuAD <sub>1.1</sub>	SQuAD <sub>2.0</sub>	Geometric mean
32	1.27 $\times$	1.42 $\times$	1.42 $\times$	1.23 $\times$	1.34 $\times$	1.36 $\times$	1.33 $\times$	1.37 $\times$	1.34 $\times$
256	1.34 $\times$	1.54 $\times$	1.53 $\times$	1.56 $\times$	1.54 $\times$	1.55 $\times$	1.34 $\times$	1.40 $\times$	1.47 $\times$

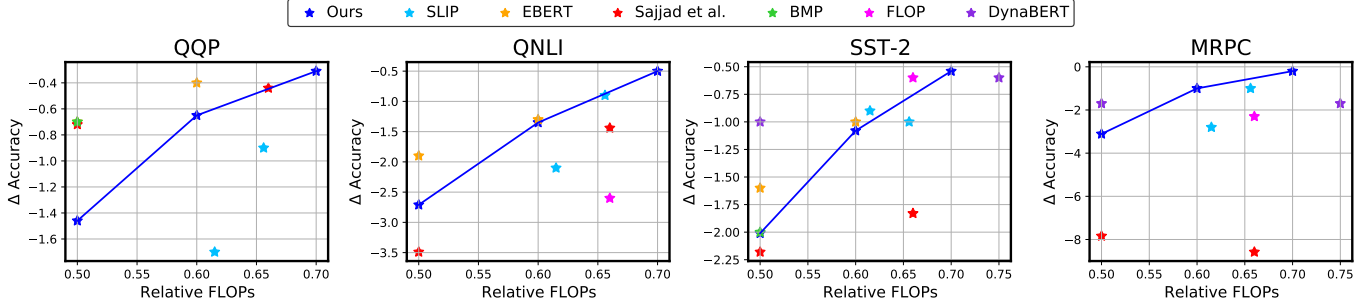


**Fig. 5:** Amount of accuracy degradation from the baseline when pruning  $BERT_{\text{BASE}}$  using our method and the prior structured pruning methods with different relative FLOPs. Note that our method does not require retraining, whereas all the other methods involve significant retraining overheads as described in Table II.

**Table II:** Comparison of end-to-end cost between the prior structured pruning methods and our method. We compare the number of training epochs and the end-to-end (E2E) time required for pruning.

	# Epochs	E2E time (hr)
DynaBERT [23]	4	12
EBERT [46]	6	5
BMP [36]	20	17
<b>Ours</b>	<b>0</b>	<b>0.01</b>

reduction (in STS-B and MRPC) even though it is already a compressed architecture.

**Latency.** We further measure the latency on real hardware by pruning  $BERT_{\text{BASE}}$  with latency constraints and deploying the resulting models on an NVIDIA V100 GPU. Table I lists the latency speedup with maximum accuracy drop of 1% for GLUE and SQuAD datasets. With batch size of 256, we achieve speedup of 1.47 $\times$  on average and up to 1.56 $\times$ .

### C. Comparison with the Prior Methods

**FLOPs and Accuracy Comparison.** Here, we compare our method with the prior structured pruning methods for Transformers including Flop [81], SLIP [71], Sajjad

et al. [59], DynaBERT [23], EBERT [46], and Block Movement Pruning (BMP) [36] by the FLOPs-accuracy trade-off of  $BERT_{\text{BASE}}$  on GLUE tasks. We use the results *without* knowledge distillation and data augmentation reported in each paper. Since the baseline accuracy differs slightly from paper to paper, we compare the amount of the accuracy drop from the baseline instead of the absolute accuracy. The results are plotted as Figure 5. We include the comparison details and full table in Section F.

Interestingly, our method exhibits comparable or sometimes better results than the prior methods *without* any model retraining and with substantially small pruning costs. This demonstrates empirically that retraining and a complex pruning pipeline is not necessary for moderate level of pruning of Transformers.

**Retraining Cost.** We select DynaBERT [23], EBERT [46], and BMT [36] that achieve comparably good accuracy in Figure 5, and we systematically analyze their end-to-end retraining costs on MNLI dataset. As shown in Table II, these methods require 5–17 hours of retraining. On the other hand, our method finishes in less than a minute, which is 2–3 orders of magnitude faster. We also highlight that this training latency only accounts for a *single* hyperparameter, and the entire cost should be multiplied by the size of the hyperparameter space. While the prior methods rely on a number of hy-

**Table III:** Ablation of our mask search, rearrangement, and tuning methods, described in Section IV. We use BERT<sub>BASE</sub> as a baseline model, and we prune with a 60% FLOPs constraint.

	MNLI	QQP	QNLI	SST-2	STS-B	MRPC	SQuAD <sub>1.1</sub>	SQuAD <sub>2.0</sub>	Avg.	Diff
Baseline	84.53	91.00	91.41	93.57	88.90	86.27	88.48	76.82		
Mask Search (Section IV-A)	81.21	89.99	88.38	92.13	87.10	83.14	82.66	71.12		
+ Mask Rearrangement (Section IV-B)	81.81	90.08	88.77	92.09	87.68	83.23	84.47	72.38	+ 0.60	
+ Mask Tuning (Section IV-C)	<b>82.51</b>	<b>90.35</b>	<b>90.06</b>	<b>92.49</b>	<b>88.00</b>	<b>85.27</b>	<b>86.72</b>	<b>75.26</b>	+ 1.27	

**Table IV:** Time breakdown (in percentage) of our pruning framework on a single NVIDIA V100 GPU. It consists of Gradient Computation (GC), Mask Search (MS, Section IV-A), Mask Rearrangement (MR, Section IV-B), and Mask Tuning (MT, Section IV-C). In the last column, we provide the total amount of time for end-to-end pruning, in seconds.

	GC	MS	MR	MT	Total (s)
GLUE	23.8%	0.3%	9.4%	66.5%	39.3
SQuAD	20.5%	0.1%	3.5%	76.0%	135.1

perparameters, ours introduce only two hyperparameters (in Section IV-C) which we fix for all experiments. See Section G for details.

Unlike other methods (including ours) that take as input the fine-tuned models, Sajjad et al. [59] starts from the pre-trained model, heuristically drops the top layers, and then fine-tunes on downstream tasks. Therefore, it can be regarded as a zero-cost pruning method. However, as can be seen in Figure 5, the resulting models suffer from large accuracy degradation in most cases.

#### D. Discussion

**Ablation Studies.** Table III lists an ablation of mask rearrangement (Section IV-B) and tuning (Section IV-C) stages for pruned BERT<sub>BASE</sub> with 60% of FLOPs. We find that both stages help recover the baseline accuracy, and that mask tuning is in particular critical, recovering up to 2.88% accuracy.

**Time Breakdown.** We break down our pruning pipeline into 4 parts—gradient computation, mask search, mask rearrangement, and mask tuning—and we measure the latency for each stage as Table IV. For GLUE and SQuAD tasks, our framework finishes in 39 and 135 seconds on average.

## VI. CONCLUSION

In this work, we have proposed a novel post-training pruning framework for Transformers that does not require model retraining. The core of our framework is the three-stage pruning that recovers the accuracy without retraining. It uses a fast Fisher-based mask search algorithm to decide which heads/filters to prune, rearranges the pruned heads/filters, and tunes the mask variables to recover the output signal for each layer. We empirically evaluate our framework using BERT<sub>BASE</sub> and DistilBERT, where our pruning method achieves up to 50% FLOPs reduction with only 1% accuracy degradation on GLUE and SQuAD datasets. This results in up to 1.56 $\times$  latency speedup on an NVIDIA V100 GPU. End-to-end pruning only needs 39 and 135 seconds for GLUE and SQuAD, which is 2–3 orders of magnitude faster than the prior methods. Overall, our method shows comparable or even better compression performance, as compared to the prior retraining-based methods.

## ACKNOWLEDGMENTS

We especially thank Suhong Moon for his fruitful feedback.

## REFERENCES

- [1] Yonathan Aflalo, Asaf Noy, Ming Lin, Itamar Friedman, and Lihi Zelnik. Knapsack pruning with inner distillation. *arXiv preprint arXiv:2002.08258*, 2020.
- [2] Alexei Baevski, Henry Zhou, Abdelrahman Mohamed, and Michael Auli. wav2vec 2.0: A framework for self-supervised learning of speech representations. *arXiv preprint arXiv:2006.11477*, 2020.
- [3] Ron Banner, Yury Nahshan, Elad Hoffer, and Daniel Soudry. Post-training 4-bit quantization of convolution networks for rapid-deployment. *arXiv preprint arXiv:1810.05723*, 2018.
- [4] Tom B Brown, Benjamin Mann, Nick Ryder, Melanie Subbiah, Jared Kaplan, Prafulla Dhariwal, Arvind Neelakantan, Pranav Shyam, Girish Sastry,

Amanda Askell, et al. Language models are few-shot learners. *arXiv preprint arXiv:2005.14165*, 2020.

[5] Daniel Cer, Mona Diab, Eneko Agirre, Inigo Lopez-Gazpio, and Lucia Specia. Semeval-2017 task 1: Semantic textual similarity-multilingual and cross-lingual focused evaluation. *arXiv preprint arXiv:1708.00055*, 2017.

[6] Daoyuan Chen, Yaliang Li, Minghui Qiu, Zhen Wang, Bofang Li, Bolin Ding, Hongbo Deng, Jun Huang, Wei Lin, and Jingren Zhou. Adabert: Task-adaptive bert compression with differentiable neural architecture search. *arXiv preprint arXiv:2001.04246*, 2020.

[7] Sanyuan Chen, Chengyi Wang, Zhengyang Chen, Yu Wu, Shujie Liu, Zhuo Chen, Jinyu Li, Naoyuki Kanda, Takuya Yoshioka, Xiong Xiao, et al. Wavlm: Large-scale self-supervised pre-training for full stack speech processing. *arXiv preprint arXiv:2110.13900*, 2021.

[8] Tianlong Chen, Jonathan Frankle, Shiyu Chang, Sijia Liu, Yang Zhang, Zhangyang Wang, and Michael Carbin. The lottery ticket hypothesis for pre-trained BERT networks. *arXiv preprint arXiv:2007.12223*, 2020.

[9] Xiaohan Chen, Yu Cheng, Shuohang Wang, Zhe Gan, Zhangyang Wang, and Jingjing Liu. Earlybert: Efficient bert training via early-bird lottery tickets. *arXiv preprint arXiv:2101.00063*, 2020.

[10] Ido Dagan, Oren Glickman, and Bernardo Magnini. The pascal recognising textual entailment challenge. In *Machine Learning Challenges Workshop*, pages 177–190. Springer, 2005.

[11] Jacob Devlin, Ming-Wei Chang, Kenton Lee, and Kristina Toutanova. Bert: Pre-training of deep bidirectional transformers for language understanding. *arXiv preprint arXiv:1810.04805*, 2018.

[12] William B Dolan and Chris Brockett. Automatically constructing a corpus of sentential paraphrases. In *Proceedings of the Third International Workshop on Paraphrasing (IWP2005)*, 2005.

[13] Alexey Dosovitskiy, Lucas Beyer, Alexander Kolesnikov, Dirk Weissenborn, Xiaohua Zhai, Thomas Unterthiner, Mostafa Dehghani, Matthias Minderer, Georg Heigold, Sylvain Gelly, et al. An image is worth 16x16 words: Transformers for image recognition at scale. *arXiv preprint arXiv:2010.11929*, 2020.

[14] Angela Fan, Edouard Grave, and Armand Joulin. Reducing transformer depth on demand with structured dropout. *arXiv preprint arXiv:1909.11556*, 2019.

[15] Jonathan Frankle and Michael Carbin. The lottery ticket hypothesis: Finding sparse, trainable neural networks. *arXiv preprint arXiv:1803.03635*, 2018.

[16] Trevor Gale, Erich Elsen, and Sara Hooker. The state of sparsity in deep neural networks. *arXiv preprint arXiv:1902.09574*, 2019.

[17] Google. Tensorflow Lite: <https://www.tensorflow.org/lite>, 2017.

[18] Tae Jun Ham, Sung Jun Jung, Seonghak Kim, Young H Oh, Yeonhong Park, Yoonho Song, Jung-Hun Park, Sanghee Lee, Kyoung Park, Jae W Lee, et al. A<sup>3</sup>: Accelerating attention mechanisms in neural networks with approximation. In *2020 IEEE International Symposium on High Performance Computer Architecture (HPCA)*, pages 328–341. IEEE, 2020.

[19] Tae Jun Ham, Yejin Lee, Seong Hoon Seo, Soosung Kim, Hyunji Choi, Sung Jun Jung, and Jae W Lee. Elsa: Hardware-software co-design for efficient, lightweight self-attention mechanism in neural networks. In *2021 ACM/IEEE 48th Annual International Symposium on Computer Architecture (ISCA)*, pages 692–705. IEEE, 2021.

[20] Yihui He, Xiangyu Zhang, and Jian Sun. Channel pruning for accelerating very deep neural networks. In *Proceedings of the IEEE international conference on computer vision*, pages 1389–1397, 2017.

[21] Dan Hendrycks and Kevin Gimpel. Gaussian error linear units (gelus). *arXiv preprint arXiv:1606.08415*, 2016.

[22] Geoffrey Hinton, Oriol Vinyals, and Jeff Dean. Distilling the knowledge in a neural network. *arXiv preprint arXiv:1503.02531*, 2015.

[23] Lu Hou, Zhiqi Huang, Lifeng Shang, Xin Jiang, Xiao Chen, and Qun Liu. Dynabert: Dynamic bert with adaptive width and depth. *arXiv preprint arXiv:2004.04037*, 2020.

[24] Wei-Ning Hsu, Benjamin Bolte, Yao-Hung Hubert Tsai, Kushal Lakhotia, Ruslan Salakhutdinov, and Abdelrahman Mohamed. Hubert: Self-supervised speech representation learning by masked prediction of hidden units. *arXiv preprint arXiv:2106.07447*, 2021.

[25] Hengyuan Hu, Rui Peng, Yu-Wing Tai, and Chi-Keung Tang. Network trimming: A data-driven neuron pruning approach towards efficient deep architectures. *arXiv preprint arXiv:1607.03250*, 2016.

[26] Itay Hubara, Yury Nahshan, Yair Hanani, Ron

Banner, and Daniel Soudry. Improving post training neural quantization: Layer-wise calibration and integer programming. *arXiv preprint arXiv:2006.10518*, 2020.

[27] Forrest N Iandola, Albert E Shaw, Ravi Krishna, and Kurt W Keutzer. Squeezebert: What can computer vision teach nlp about efficient neural networks? *arXiv preprint arXiv:2006.11316*, 2020.

[28] Intel. OpenVINO: <https://docs.openvino.ai/latest/index.html>, 2021.

[29] Shankar Iyer, Nikhil Dandekar, and Kornl Csernai. First quora dataset release: Question pairs.(2017). URL <https://data.quora.com/First-Quora-Dataset-Release-Question-Pairs>, 2017.

[30] Xiaoqi Jiao, Yichun Yin, Lifeng Shang, Xin Jiang, Xiao Chen, Linlin Li, Fang Wang, and Qun Liu. Tinybert: Distilling bert for natural language understanding. *arXiv preprint arXiv:1909.10351*, 2019.

[31] Ashish Khetan and Zohar Karnin. schubert: Optimizing elements of bert. *arXiv preprint arXiv:2005.06628*, 2020.

[32] Sehoon Kim, Amir Gholami, Zhewei Yao, Michael W Mahoney, and Kurt Keutzer. I-bert: Integer-only bert quantization. *arXiv preprint arXiv:2101.01321*, 2021.

[33] Woojeong Kim, Suhyun Kim, Mincheol Park, and Geonseok Jeon. Neuron merging: Compensating for pruned neurons. *arXiv preprint arXiv:2010.13160*, 2020.

[34] Nikita Kitaev, Lukasz Kaiser, and Anselm Levskaya. Reformer: The efficient transformer. In *International Conference on Learning Representations*, 2019.

[35] Woosuk Kwon, Gyeong-In Yu, Eunji Jeong, and Byung-Gon Chun. Nimble: Lightweight and parallel gpu task scheduling for deep learning. *arXiv preprint arXiv:2012.02732*, 2020.

[36] François Lagunas, Ella Charlaix, Victor Sanh, and Alexander M Rush. Block pruning for faster transformers. *arXiv preprint arXiv:2109.04838*, 2021.

[37] Zhenzhong Lan, Mingda Chen, Sebastian Goodman, Kevin Gimpel, Piyush Sharma, and Radu Soricut. Albert: A lite bert for self-supervised learning of language representations. *arXiv preprint arXiv:1909.11942*, 2019.

[38] Yann LeCun, John S Denker, and Sara A Solla. Optimal brain damage. In *Advances in neural information processing systems*, pages 598–605, 1990.

[39] Hector Levesque, Ernest Davis, and Leora Morgenstern. The winograd schema challenge. In *Thirteenth International Conference on the Principles of Knowledge Representation and Reasoning*. Citeseer, 2012.

[40] Bingbing Li, Zhenglun Kong, Tianyun Zhang, Ji Li, Zhengang Li, Hang Liu, and Caiwen Ding. Efficient transformer-based large scale language representations using hardware-friendly block structured pruning. *arXiv preprint arXiv:2009.08065*, 2020.

[41] Zi Lin, Jeremiah Zhe Liu, Zi Yang, Nan Hua, and Dan Roth. Pruning redundant mappings in transformer models via spectral-normalized identity prior. *arXiv preprint arXiv:2010.01791*, 2020.

[42] Liyang Liu, Shilong Zhang, Zhanghui Kuang, Aojun Zhou, Jing-Hao Xue, Xinjiang Wang, Yimin Chen, Wenming Yang, Qingmin Liao, and Wayne Zhang. Group fisher pruning for practical network compression. In *International Conference on Machine Learning*, pages 7021–7032. PMLR, 2021.

[43] Yinhan Liu, Myle Ott, Naman Goyal, Jingfei Du, Mandar Joshi, Danqi Chen, Omer Levy, Mike Lewis, Luke Zettlemoyer, and Veselin Stoyanov. Roberta: A robustly optimized bert pretraining approach. *arXiv preprint arXiv:1907.11692*, 2019.

[44] Yuanxin Liu, Zheng Lin, and Fengcheng Yuan. Rosita: Refined bert compression with integrated techniques. In *Proceedings of the AAAI Conference on Artificial Intelligence*, volume 35, pages 8715–8722, 2021.

[45] Ze Liu, Yutong Lin, Yue Cao, Han Hu, Yixuan Wei, Zheng Zhang, Stephen Lin, and Baining Guo. Swin transformer: Hierarchical vision transformer using shifted windows. *arXiv preprint arXiv:2103.14030*, 2021.

[46] Zejian Liu, Fanrong Li, Gang Li, and Jian Cheng. Ebert: Efficient bert inference with dynamic structured pruning. In *Findings of the Association for Computational Linguistics: ACL-IJCNLP 2021*, pages 4814–4823, 2021.

[47] Lingxiao Ma, Zhiqiang Xie, Zhi Yang, Jilong Xue, Youshan Miao, Wei Cui, Wenxiang Hu, Fan Yang, Lintao Zhang, and Lidong Zhou. Rammer: Enabling holistic deep learning compiler optimizations with rtasks. In *14th {USENIX} Symposium on Operating Systems Design and Implementation ({OSDI} 20)*, pages 881–897, 2020.

[48] Paul Michel, Omer Levy, and Graham Neubig. Are sixteen heads really better than one? *arXiv preprint arXiv:1905.10650*, 2019.

[49] Seyed Iman Mirzadeh, Mehrdad Farajtabar, Ang

Li, Nir Levine, Akihiro Matsukawa, and Hassan Ghasemzadeh. Improved knowledge distillation via teacher assistant. In *Proceedings of the AAAI Conference on Artificial Intelligence*, volume 34, pages 5191–5198, 2020.

[50] Pavlo Molchanov, Arun Mallya, Stephen Tyree, Iuri Frosio, and Jan Kautz. Importance estimation for neural network pruning. In *Proceedings of the IEEE/CVF Conference on Computer Vision and Pattern Recognition*, pages 11264–11272, 2019.

[51] Markus Nagel, Rana Ali Amjad, Mart Van Baalen, Christos Louizos, and Tijmen Blankevoort. Up or down? adaptive rounding for post-training quantization. In *International Conference on Machine Learning*, pages 7197–7206. PMLR, 2020.

[52] ROYUD Nishino and Shohei Hido Crissman Loomis. Cupy: A numpy-compatible library for nvidia gpu calculations. *31st conference on neural information processing systems*, 151, 2017.

[53] NVIDIA. TensorRT: <https://developer.nvidia.com/tensorrt>, 2018.

[54] Adam Paszke, Sam Gross, Francisco Massa, Adam Lerer, James Bradbury, Gregory Chanan, Trevor Killeen, Zeming Lin, Natalia Gimelshein, Luca Antiga, et al. Pytorch: An imperative style, high-performance deep learning library. *Advances in neural information processing systems*, 32:8026–8037, 2019.

[55] Sai Prasanna, Anna Rogers, and Anna Rumshisky. When BERT plays the lottery, all tickets are winning. *arXiv preprint arXiv:2005.00561*, 2020.

[56] Valentin Radu, Kuba Kaszyk, Yuan Wen, Jack Turner, José Cano, Elliot J Crowley, Björn Franke, Amos Storkey, and Michael O’Boyle. Performance aware convolutional neural network channel pruning for embedded gpus. In *2019 IEEE International Symposium on Workload Characterization (IISWC)*, pages 24–34. IEEE, 2019.

[57] Pranav Rajpurkar, Robin Jia, and Percy Liang. Know what you don’t know: Unanswerable questions for squad. *arXiv preprint arXiv:1806.03822*, 2018.

[58] Pranav Rajpurkar, Jian Zhang, Konstantin Lopyrev, and Percy Liang. SQuAD: 100,000+ questions for machine comprehension of text. *arXiv preprint arXiv:1606.05250*, 2016.

[59] Hassan Sajjad, Fahim Dalvi, Nadir Durrani, and Preslav Nakov. On the effect of dropping layers of pre-trained transformer models. *arXiv preprint arXiv:2004.03844*, 2020.

[60] Victor Sanh, Lysandre Debut, Julien Chaumond, and Thomas Wolf. Distilbert, a distilled version of bert: smaller, faster, cheaper and lighter. *arXiv preprint arXiv:1910.01108*, 2019.

[61] Victor Sanh, Thomas Wolf, and Alexander M Rush. Movement pruning: Adaptive sparsity by fine-tuning. *arXiv preprint arXiv:2005.07683*, 2020.

[62] Maying Shen, Hongxu Yin, Pavlo Molchanov, Lei Mao, Jianna Liu, and Jose M Alvarez. Halp: Hardware-aware latency pruning. *arXiv preprint arXiv:2110.10811*, 2021.

[63] Sheng Shen, Zhen Dong, Jiayu Ye, Linjian Ma, Zhewei Yao, Amir Gholami, Michael W Mahoney, and Kurt Keutzer. Q-bert: Hessian based ultra low precision quantization of bert. In *Proceedings of the AAAI Conference on Artificial Intelligence*, volume 34, pages 8815–8821, 2020.

[64] David So, Quoc Le, and Chen Liang. The evolved transformer. In *International Conference on Machine Learning*, pages 5877–5886. PMLR, 2019.

[65] David R So, Wojciech Mańke, Hanxiao Liu, Zihang Dai, Noam Shazeer, and Quoc V Le. Primer: Searching for efficient transformers for language modeling. *arXiv preprint arXiv:2109.08668*, 2021.

[66] Richard Socher, Alex Perelygin, Jean Wu, Jason Chuang, Christopher D Manning, Andrew Y Ng, and Christopher Potts. Recursive deep models for semantic compositionality over a sentiment treebank. In *Proceedings of the 2013 conference on empirical methods in natural language processing*, pages 1631–1642, 2013.

[67] Suraj Srinivas and R Venkatesh Babu. Data-free parameter pruning for deep neural networks. *arXiv preprint arXiv:1507.06149*, 2015.

[68] Siqi Sun, Yu Cheng, Zhe Gan, and Jingjing Liu. Patient knowledge distillation for bert model compression. *arXiv preprint arXiv:1908.09355*, 2019.

[69] Zhiqing Sun, Hongkun Yu, Xiaodan Song, Renjie Liu, Yiming Yang, and Denny Zhou. Mobilebert: a compact task-agnostic bert for resource-limited devices. *arXiv preprint arXiv:2004.02984*, 2020.

[70] Thierry Tambe, Coleman Hooper, Lillian Pentecost, Tianyu Jia, En-Yu Yang, Marco Donato, Victor Sanh, Paul Whatmough, Alexander M Rush, David Brooks, et al. Edgebert: Sentence-level energy optimizations for latency-aware multi-task nlp inference. In *MICRO-54: 54th Annual IEEE/ACM International Symposium on Microarchitecture*, pages 830–844, 2021.

[71] Hidenori Tanaka, Daniel Kunin, Daniel LK Yamins, and Surya Ganguli. Pruning neural networks without

any data by iteratively conserving synaptic flow. *arXiv preprint arXiv:2006.05467*, 2020.

[72] Lucas Theis, Iryna Korshunova, Alykhan Tejani, and Ferenc Huszár. Faster gaze prediction with dense networks and fisher pruning. *arXiv preprint arXiv:1801.05787*, 2018.

[73] Hugo Touvron, Matthieu Cord, Matthijs Douze, Francisco Massa, Alexandre Sablayrolles, and Hervé Jégou. Training data-efficient image transformers & distillation through attention. In *International Conference on Machine Learning*, pages 10347–10357. PMLR, 2021.

[74] Ashish Vaswani, Noam Shazeer, Niki Parmar, Jakob Uszkoreit, Llion Jones, Aidan N Gomez, Łukasz Kaiser, and Illia Polosukhin. Attention is all you need. In *Advances in neural information processing systems*, pages 5998–6008, 2017.

[75] Elena Voita, David Talbot, Fedor Moiseev, Rico Sennrich, and Ivan Titov. Analyzing multi-head self-attention: Specialized heads do the heavy lifting, the rest can be pruned. *arXiv preprint arXiv:1905.09418*, 2019.

[76] Alex Wang, Amanpreet Singh, Julian Michael, Felix Hill, Omer Levy, and Samuel R Bowman. GLUE: A multi-task benchmark and analysis platform for natural language understanding. *arXiv preprint arXiv:1804.07461*, 2018.

[77] Hanrui Wang, Zhanghao Wu, Zhijian Liu, Han Cai, Ligeng Zhu, Chuang Gan, and Song Han. Hat: Hardware-aware transformers for efficient natural language processing. *arXiv preprint arXiv:2005.14187*, 2020.

[78] Hanrui Wang, Zhekai Zhang, and Song Han. Spatten: Efficient sparse attention architecture with cascade token and head pruning. In *2021 IEEE International Symposium on High-Performance Computer Architecture (HPCA)*, pages 97–110. IEEE, 2021.

[79] Sinong Wang, Belinda Li, Madian Khabsa, Han Fang, and Hao Ma. Linformer: Self-attention with linear complexity. *arXiv preprint arXiv:2006.04768*, 2020.

[80] Wenhui Wang, Furu Wei, Li Dong, Hangbo Bao, Nan Yang, and Ming Zhou. Minilm: Deep self-attention distillation for task-agnostic compression of pre-trained transformers. *arXiv preprint arXiv:2002.10957*, 2020.

[81] Ziheng Wang, Jeremy Wohlwend, and Tao Lei. Structured pruning of large language models. *arXiv preprint arXiv:1910.04732*, 2019.

[82] Alex Warstadt, Amanpreet Singh, and Samuel R Bowman. Neural network acceptability judgments. *Transactions of the Association for Computational Linguistics*, 7:625–641, 2019.

[83] Adina Williams, Nikita Nangia, and Samuel R Bowman. A broad-coverage challenge corpus for sentence understanding through inference. *arXiv preprint arXiv:1704.05426*, 2017.

[84] Thomas Wolf, Julien Chaumond, Lysandre Debut, Victor Sanh, Clement Delangue, Anthony Moi, Pierrick Cistac, Morgan Funtowicz, Joe Davison, Sam Shleifer, et al. Transformers: State-of-the-art natural language processing. In *Proceedings of the 2020 Conference on Empirical Methods in Natural Language Processing: System Demonstrations*, pages 38–45, 2020.

[85] Zhanghao Wu, Zhijian Liu, Ji Lin, Yujun Lin, and Song Han. Lite transformer with long-short range attention. *arXiv preprint arXiv:2004.11886*, 2020.

[86] Jin Xu, Xu Tan, Renqian Luo, Kaitao Song, Jian Li, Tao Qin, and Tie-Yan Liu. Nas-bert: Task-agnostic and adaptive-size bert compression with neural architecture search. *arXiv preprint arXiv:2105.14444*, 2021.

[87] Zhewei Yao, Linjian Ma, Sheng Shen, Kurt Keutzer, and Michael W Mahoney. Mlpruning: A multilevel structured pruning framework for transformer-based models. *arXiv preprint arXiv:2105.14636*, 2021.

[88] Yichun Yin, Cheng Chen, Lifeng Shang, Xin Jiang, Xiao Chen, and Qun Liu. Autotinybert: Automatic hyper-parameter optimization for efficient pre-trained language models. *arXiv preprint arXiv:2107.13686*, 2021.

[89] Ali Hadi Zadeh, Isak Edo, Omar Mohamed Awad, and Andreas Moshovos. Gobo: Quantizing attention-based nlp models for low latency and energy efficient inference. In *2020 53rd Annual IEEE/ACM International Symposium on Microarchitecture (MICRO)*, pages 811–824. IEEE, 2020.

[90] Ofir Zafrir, Guy Boudoukh, Peter Izsak, and Moshe Wasserblat. Q8bert: Quantized 8bit bert. *arXiv preprint arXiv:1910.06188*, 2019.

[91] Ritchie Zhao, Yuwei Hu, Jordan Dotzel, Christopher De Sa, and Zhiru Zhang. Improving neural network quantization without retraining using outlier channel splitting. *Proceedings of Machine Learning Research*, 2019.

## APPENDIX

### A. Proof of Equation 12

We prove Eq. 12 by contradiction. Suppose that there exists a mask  $m$  such that

$$\sum_{i \in Z(m)} \mathcal{I}_{ii} < \sum_{i \in Z(m^*)} \mathcal{I}_{ii}, \quad (16)$$

where the mask  $m^*$  is the output of Algorithm 1. Let  $h = \|m^{\text{MHA}}\|_0$ , i.e. the total number of heads in the architecture pruned by the mask  $m$ . Then we construct a new mask  $m'$  as follows:

- 1) Keep the mask for MHA layers. That is,  $m'^{\text{MHA}} = m^{\text{MHA}}$ .
- 2) Construct  $m'^{\text{FFN}}$  as in the inner statements of the for loop (line 1 of Algorithm 1). That is, given a mask initialized to 1, we zero out the  $k$  filter mask variables with the least important scores, where  $k = NL - \lfloor (C - fF_{\text{head}})/F_{\text{filter}} \rfloor$ .

Obviously, the mask  $m'$  satisfies the FLOPs constraint Eq. 11. Moreover, as the mask  $m'$  prunes the least important filters, the following two inequalities hold:

$$\sum_{i \in Z(m'^{\text{FFN}})} \mathcal{I}_{ii} \leq \sum_{i \in Z(m^{\text{FFN}})} \mathcal{I}_{ii}, \quad (17)$$

$$\sum_{i \in Z(m')} \mathcal{I}_{ii} = \sum_{i \in Z(m'^{\text{MHA}})} \mathcal{I}_{ii} + \sum_{i \in Z(m'^{\text{FFN}})} \mathcal{I}_{ii} \leq \sum_{i \in Z(m^{\text{MHA}})} \mathcal{I}_{ii} + \sum_{i \in Z(m^{\text{FFN}})} \mathcal{I}_{ii} = \sum_{i \in Z(m)} \mathcal{I}_{ii}. \quad (18)$$

Then we construct another mask  $m^*$  from  $m'$  such that:

- 1) Keep the mask for FFN layers. That is,  $m'^{\text{FFN}} = m^{\text{FFN}}$ .
- 2) Construct  $m'^{\text{MHA}}$  by zeroing out  $h$  head mask variables with the least important scores from a mask initialized to 1.

Due to the observation (2) in Section IV-A, the following inequalities hold:

$$\sum_{i \in Z(m'^{\text{MHA}})} \mathcal{I}_{ii} \leq \sum_{i \in Z(m^{\text{MHA}})} \mathcal{I}_{ii}, \quad (19)$$

$$\sum_{i \in Z(m^*)} \mathcal{I}_{ii} = \sum_{i \in Z(m'^{\text{MHA}})} \mathcal{I}_{ii} + \sum_{i \in Z(m'^{\text{FFN}})} \mathcal{I}_{ii} \leq \sum_{i \in Z(m^{\text{MHA}})} \mathcal{I}_{ii} + \sum_{i \in Z(m^{\text{FFN}})} \mathcal{I}_{ii} = \sum_{i \in Z(m')} \mathcal{I}_{ii}. \quad (20)$$

Essentially,  $m^*$  is the mask when  $n$  (in line 1 of Algorithm 1) is  $h$ . As Algorithm 1 finds the minimum by iterating different values of  $n$ , the following inequalities hold:

$$\sum_{i \in Z(m^*)} \mathcal{I}_{ii} \leq \sum_{i \in Z(m^*)} \mathcal{I}_{ii}. \quad (21)$$

Finally, the above inequalities are combined as follows:

$$\sum_{i \in Z(m^*)} \mathcal{I}_{ii} \leq \sum_{i \in Z(m^*)} \mathcal{I}_{ii} \leq \sum_{i \in Z(m')} \mathcal{I}_{ii} \leq \sum_{i \in Z(m)} \mathcal{I}_{ii}, \quad (22)$$

which contradicts Eq. 16. Thus, the output mask  $m^*$  of Algorithm 1 is the minimizer of Eq. 10.  $\square$

### B. Latency-aware Search Algorithm

Algorithm 2 is our proposed algorithm for latency-aware mask search, which extends Algorithm 1. It takes as inputs the given latency constraint, approximated LAT functions for MHA and FFN layers, and the diagonal Fisher information matrix  $\mathcal{I}$ . Overall, Algorithm 2 has the same structure as Algorithm 1. A notable difference between the two is that Algorithm 2 separately considers the constant part (i.e., when the number of heads/filters is below the threshold  $T$ ) in line 1–5. Another difference is that Algorithm 2 uses  $a_{\text{head}}$  and  $a_{\text{filter}}$  instead of  $F_{\text{head}}$  and  $F_{\text{filter}}$  in Algorithm 1.

---

**Algorithm 2** Mask Search with a Latency Constraint

---

**Input:** Latency constraint  $C$ , LAT function parameters  $(a_{\text{head}}, c_{\text{head}}, T_{\text{head}}), (a_{\text{filter}}, c_{\text{filter}}, T_{\text{filter}})$ , diagonal Fisher information matrix  $\mathcal{I}$

- 1: HI = indicies pf  $T_{\text{head}}$  most important heads in each layer
- 2: FI = indicies of  $T_{\text{filter}}$  most important filters in each layer
- 3:  $H' = H - T_{\text{head}}$
- 4:  $N' = N - T_{\text{filter}}$
- 5:  $C' = C - L(c_{\text{head}} + c_{\text{filter}})$
- 6: **for**  $n = 0$  **to**  $H'L$  **do**
- 7:    $I$  = indicies of  $n$  most important heads not in HI
- 8:    $f = \lfloor (C' - na_{\text{head}})/a_{\text{filter}} \rfloor$
- 9:    $J$  = indicies of  $f$  most important filters not in FI
- 10:    $\text{HI}' = \text{HI} \cup I$
- 11:    $\text{FI}' = \text{FI} \cup J$
- 12:    $S[n] = \sum_{i \in \text{HI}' \cup \text{FI}'} \mathcal{I}_{ii}$
- 13:    $R[n] = (\text{HI}', \text{FI}')$
- 14: **end for**
- 15:  $n^* = \arg \max_n S[n]$
- 16:  $\text{HI}^*, \text{FI}^* = R[n^*]$
- 17: Initialize  $\mathbf{m}^{\text{MHA}}$  and  $\mathbf{m}^{\text{FFN}}$  as 0
- 18:  $\mathbf{m}^{\text{MHA}}[\text{HI}^*] = 1$
- 19:  $\mathbf{m}^{\text{FFN}}[\text{FI}^*] = 1$

**Output:**  $\mathbf{m}^* = (\mathbf{m}^{\text{MHA}}, \mathbf{m}^{\text{FFN}})$

---

### C. Derivation of Equation 14

Based on Eq. 6 and the warm-start constraint in Section IV-B, the optimization problem Eq. 5 is written as follows:

$$\arg \min_{\mathbf{m}} (\mathbf{1} - \mathbf{m})^\top \mathcal{I} (\mathbf{1} - \mathbf{m}), \quad (23)$$

$$\text{s.t. } \|\mathbf{m}_l\|_0 = \|\mathbf{m}_l^*\|_0 \text{ for } l = 1, 2, \dots, L, \quad (24)$$

where  $\mathbf{m}^*$  is the mask searched in Section IV-A using the diagonal approximation of  $\mathcal{I}$ . Under the block diagonal assumption, Eq. 23 can be reduced as follows:

$$\arg \min_{\mathbf{m}} (\mathbf{1} - \mathbf{m})^\top \mathcal{I} (\mathbf{1} - \mathbf{m}) \approx \arg \min_{\mathbf{m}} \sum_{l=1}^L (\mathbf{1} - \mathbf{m}_l)^\top \mathcal{I}_l (\mathbf{1} - \mathbf{m}_l), \quad (25)$$

where  $\mathcal{I}_l$  is the  $l$ -th diagonal block of  $\mathcal{I}$ . Here what we want to show is that the problem Eq. 25 can be solved by independently solving the optimization problem Eq. 14 for each layer. We prove this by contradiction. Suppose that  $\hat{\mathbf{m}} = (\hat{\mathbf{m}}_1, \dots, \hat{\mathbf{m}}_L)$  is the mask obtained by solving Eq. 14 for each layer. If there exists a mask  $\mathbf{m}$  that strictly better optimizes Eq. 25 than  $\hat{\mathbf{m}}$ :

$$\sum_{l=1}^L (\mathbf{1} - \mathbf{m}_l)^\top \mathcal{I}_l (\mathbf{1} - \mathbf{m}_l) < \sum_{l=1}^L (\mathbf{1} - \hat{\mathbf{m}}_l)^\top \mathcal{I}_l (\mathbf{1} - \hat{\mathbf{m}}_l), \quad (26)$$

while also satisfying the constraint Eq. 24, then there must exist a layer  $k$  such that

$$(\mathbf{1} - \mathbf{m}_k)^\top \mathcal{I}_k (\mathbf{1} - \mathbf{m}_k) < (\mathbf{1} - \hat{\mathbf{m}}_k)^\top \mathcal{I}_k (\mathbf{1} - \hat{\mathbf{m}}_k). \quad (27)$$

However, this contradicts the assumption that  $\hat{\mathbf{m}}_k$  is the minimizer of Eq. 14 for layer  $k$ . Therefore, such a mask as  $\mathbf{m}$  cannot exist, and  $\hat{\mathbf{m}}_k$  is the optimal solution for Eq. 25.

### D. Formulating Equation 15 as a Linear Least Squares Problem

For an MHA layer, the problem of minimizing reconstruction error can be written as follows:

$$\arg \min_{\mathbf{m}_l^{\text{MHA}}} \|(\mathbf{x} + \text{MHA}(\mathbf{x}; \mathbf{m}_l^{\text{MHA}})) - (\mathbf{x}' + \text{MHA}(\mathbf{x}'; \mathbf{1}))\|_2^2, \quad (28)$$

$$\text{s.t. } Z(\mathbf{m}_l^{\text{MHA}}) = Z(\hat{\mathbf{m}}_l^{\text{MHA}}), \quad (29)$$

where  $\hat{m}$  is the mask obtained as the result of mask rearrangement (Section IV-B). Eq. 29 is the constraint we impose in Section IV-C that the zero-valued mask variables in  $\hat{m}$  are fixed to 0 so that the tuned mask also satisfies the FLOPs/latency constraint. Then we rewrite the problem as the following linear least squares problem:

$$\arg \min_{m_l} \|A m_l - b\|_2^2, \quad (30)$$

$$\text{where } A := [\hat{m}_{l,1}^{\text{MHA}} \text{Att}_1(x), \dots, \hat{m}_{l,H}^{\text{MHA}} \text{Att}_H(x)] \text{ and } b := (x' + \sum_{h=1}^H \text{Att}_h(x')) - x. \quad (31)$$

Here, the elements of  $\hat{m}_l^{\text{MHA}}$  are multiplied to the matrix  $A$  to ensure that the output activations of the pruned heads are not used to reconstruct the original output. Although Eq. 30 has a closed form solution  $(A^T A)^{-1} A^T B$ , we use the numerical solver in CuPy for higher stability.

### E. Experimental Details

1) *Experimental Setup*: Our framework is implemented on top of PyTorch v1.9.1 [54] and HuggingFace Transformers v4.12.0 [84]. For the baseline, we downloaded the pre-trained checkpoints from the HuggingFace Transformers repository, and we fine-tuned them on GLUE [76] and SQuAD [57, 58] datasets with the standard training recipe. We then use 2K examples from the training sets to prune the baseline models. We report accuracy for GLUE tasks, except for STS-B that we report Spearman Correlation, and F1 score for SQuAD tasks on the development sets. All experiments in this paper are conducted on an AWS p3.2xlarge instance which has an NVIDIA V100 GPU. We used seed numbers from 0 to 9, and we reported the averaged results.

2) *Datasets*: GLUE tasks [76] include sentence similarity (QQP [29], MRPC [12], STS-B [5]), sentiment classification (SST-2 [66]), textual entailment (RTE [10]) and natural language inference (MNLI [83], QNLI [58]). There are 364K, 4K, 6K, 67K, 3K, 392K, 105K training examples, respectively. We exclude CoLA [82] and WLNI [39] due to their unstable behaviors.

SQuAD 1.1 [58] and SQuAD 2.0 [57] are question and answering tasks, each of which contains 88K and 130K training examples. SQuAD 2.0 is an extension of SQuAD 1.1 by including unanswerable questions whose answers are not stated in the given contexts.

### F. Details for the Comparison with the Prior Methods

We compare the FLOPs-accuracy trade-off of our method to the prior structured pruning methods for Transformers in Flop [81], SLIP [71], Sajjad et al. [59], DynaBERT [23], EBERT [46], and Block Movement Pruning (BMP) [36] on 4 GLUE tasks, QQP, QNLI, SST-2, and MRPC. We use the FLOPs and accuracy values reported in each paper (for Flop, we use the values reported in SLIP). To make a fair comparison, we use the experimental results *without* any additional knowledge distillation or data augmentation in each paper. Because all of these papers have slight differences in their baseline accuracy, it is difficult to directly compare the absolute accuracy for the pruned models. Therefore, we use the amount of the accuracy drop (i.e., accuracy of the pruned model subtracted by the accuracy of the original model) instead. For Flop and SLIP, the results for MRPC are reported as F1 score instead of accuracy. For these cases, we report that the amount of the F1 score drop instead, assuming that it is similar to the amount of the accuracy drop. Since BMP only reports the parameter counts reduction, we directly use this value as FLOPs reduction, under an assumption that the head pruning ratio is similar to the filter pruning ratio. We include the full table in Table V.

### G. Retraining Costs

DynaBERT [23] consists of 2-stage training, 1 epoch of width and depth-adaptive training followed by additional 3 epochs of final fine-tuning. For the first stage, it jointly trains 12 different width and depth configurations, roughly adding up 12 $\times$  training costs than the normal training. EBERT [46] consists of 2-stage training, 3 epochs that jointly trains the pruning parameters and the model weights, followed by 3 additional epochs of final fine-tuning. BMT [36] requires 20 epochs of training to search for the optimal pruning configuration and retrain the model weights. We measure end-to-end retraining latency on an NVIDIA V100 GPU using a batch size of 32 for all experiments.

**Table V:** The absolute accuracy and the amount of accuracy degradation from the baseline after pruning BERT<sub>BASE</sub> using our method and the prior structured pruning methods with different relative FLOPs. <sup>†</sup>Reported as F1 score instead of accuracy.

Method	Rel. FLOPs	Accuracy				Accuracy Diff			
		QQP	QNLI	SST-2	MRPC	QQP	QNLI	SST-2	MRPC
Flop [81]	Baseline	-	91.6	92.7	90.9 <sup>†</sup>	-	0	0	0
	66.7	-	89.0	92.1	88.6 <sup>†</sup>	-	-2.6	-0.6	-2.3
SLIP [71]	Baseline	90.6	91.6	92.7	90.9 <sup>†</sup>	0	0	0	0
	65.6	89.7	90.7	91.7	89.9 <sup>†</sup>	-0.9	-0.9	-1.0	-1.0
	61.5	88.9	89.5	91.8	88.1 <sup>†</sup>	-1.7	-2.1	-0.9	-2.8
Sajjad et al. [59]	Baseline	91.1	91.1	92.4	88.0	0	0	0	0
	66.7	90.6	89.7	90.6	79.4	-0.4	-1.4	-1.8	-8.6
	50.0	90.4	87.6	90.3	80.2	-0.7	-3.5	-2.2	-7.8
DynaBERT [23]	Baseline	-	-	92.9	87.7	-	-	0	0
	75.0	-	-	92.3	86.0	-	-	-0.6	-1.7
	50.0	-	-	91.9	86.0	-	-	-1.0	-1.7
EBERT [46]	Baseline	87.9	91.5	93.2	-	0	0	0	-
	60.0	87.5	90.2	92.2	-	-0.4	-1.3	-1.0	-
	50.0	87.0	89.6	91.6	-	-0.7	-1.9	-1.6	-
BMP [36]	Baseline	91.1	-	92.7	-	0	-	0	-
	50.0	90.4	-	90.7	-	-0.7	-	-2.0	-
Ours	Baseline	91.0	91.4	93.6	86.3	0	0	0	0
	70.0	90.7	90.9	93.0	86.1	-0.3	-0.5	-0.6	-0.2
	60.0	90.4	90.0	92.5	85.3	-0.6	-1.4	-1.1	-1.0
	50.0	89.5	88.7	91.6	83.2	-1.5	-2.7	-2.0	-3.1